with increasing frequency at doses approaching or exceeding the median lethal dose ($LD_{50}$). Thus, the benzoquinolinediones displayed teratogenic activity over a range of doses. At higher doses the abnormalities were severe and the embryos died, whereas at lower doses of the range, embryos survived to emerge with visible evidence of teratogenicity in the form of extra body structures or distally duplicated appendages. Indeed, the highest percentages of multiple-eyed embryos were seen at doses of **1** producing low mortality (Table 1).

Subsequent isolation and characterization of the impurities in commercial acridine have demonstrated the presence of **1** in the teratogenic mixture and have confirmed the identification by gas chromatography–mass spectrometry and by infrared and $^{13}C$ nuclear magnetic resonance spectra (*7*). Whether **1** is also responsible for the teratogenic activity of the other organic mixtures tested on cricket embryos is not known at this time.

Bioassays of molecules structurally similar to **1** and **2** illustrate the unique teratogenic properties of the two $C_{13}H_7NO_2$ isomers (molecular weight, 209) and establish the critical contributions of the two keto groups and the nitrogen atom in conferring morphogenetic activity. None of the eight three-ringed aromatic isomers of $C_{13}H_9N$ (molecular weight, 179) produced extra body structures, although embryotoxicity was observed with all of the isomers; this shows that the lack of teratogenicity was not caused by an inability to penetrate the egg (*7*). In addition, benzo[*g*]quinoline-5,10-dione ($C_{13}H_7NO_2$; molecular weight, 209), which differs from **1** only by the position of nitrogen in the ring, lacked teratogenic activity (*8*), further indicating that slight changes in chemical structure resulted in loss of teratogenicity.

Compound **1** proved to be more embryotoxic than **2**. On the basis of the data in Table 1, the $LD_{50}$ for **1** is 13.2 ng per egg (95 percent confidence limits of 12.6 and 14.2 ng per egg), and the $LD_{50}$ of **2** is 85.3 ng per egg (95 percent confidence limits of 74.1 and 98.3 ng per egg) (*9*). Extra compound eyes were not observed in the 1380 control eggs used in this study, nor in any of the 50,781 control eggs examined in earlier studies of chemical teratogenesis in *A. domesticus* (*1*, *2*).

The cricket *A. domesticus* provides numerous advantages as a research animal for embryology. It is easily obtained and reared; the eggs are relatively large, with less than 2 weeks required to complete development; and considerable information is available on embryonic development (*10*). The demonstrated abilities of certain benzoquinolinediones to induce extra body structures in this insect, as well as to disrupt embryonic morphogenesis in the moth *Manduca sexta* (L.), the bug *Pyrrhocoris apterus* (*11*), and the cricket *Gryllus rubens* Scudder (*12*), indicate that these chemicals will be useful tools for exploring the processes of embryonic cellular differentiation, pattern formation, and chemically induced teratogenesis. We propose that the more potent insect teratogen, benz[*g*]isoquinoline-5,10-dione, be called "biquidone," a shortened version of the full chemical name.

BARBARA T. WALTON
*Environmental Sciences Division,*
*Oak Ridge National Laboratory,*
*Oak Ridge, Tennessee 37830*

C.-H. HO
C. Y. MA
*Analytical Chemistry Division,*
*Oak Ridge National Laboratory*

E. G. O'NEILL
*Environmental Sciences Division,*
*Oak Ridge National Laboratory*

G. L. KAO
*Analytical Chemistry Division,*
*Oak Ridge National Laboratory*

### References and Notes

1. Chemical induction of duplicated body structures in crickets occurred after eggs were treated with liquids produced by several coal liquefaction processes, ether-soluble bases isolated from a coal liquid, and soil contaminated by a coal liquid spill [B. T. Walton, M. V. Buchanan, C.-h. Ho, in *Energy and Environmental Chemistry*, L. H. Keith, Ed. (Ann Arbor Science, Ann Arbor, Mich., 1982), vol. 1, p. 249; R. F. Strayer, N. T. Edwards, B. T. Walton, V. Charles-Shannon, *Environ. Toxicol. Chem.*, in press].
2. B. T. Walton, *Science* **212**, 51 (1981).
3. ———, *Fundam. Appl. Toxicol.*, in press.
4. A. Philips, *Chem. Ber.* **27**, 1923 (1894); Zd. H. Skraup and A. Cobenzl, *Monatshefte* **4**, 436 (1883). Each isomer was purified by high-performance liquid chromatography to 99 percent or more. Structures were confirmed with mass spectrometry and with infrared and $^{13}C$ nuclear magnetic resonance spectra.
5. A Hamilton syringe attached to a power-driven micrometer was used to apply 0.05 μl of various chemicals dissolved in dimethyl sulfoxide to eggs at 16 to 24 hours after oviposition. Eggs were incubated at 31°C on moist filter paper in covered petri plates (20 eggs per plate). The eggs were scored for multiple eyespots on days 8 to 11 of development.
6. The acridine used in these experiments, which contained less than 2 percent impurities, was prepared by vacuum distillation of coal tar (A. Bader, Aldrich Chemical Company, personal communication).
7. C. Y. Ma, C.-h. Ho, B. T. Walton, G. L. Kao, M. Guerin, in preparation. The isolation of the teratogenic impurity from commercial acridine samples and its identification as benz[*g*]isoquinoline-5,10-dione was reported at the March 1983 meeting of the Society of Toxicology [C.-h. Ho, C. Y. Ma, B. T. Walton, M. R. Guerin, *Toxicologist* **3**, 29 (1983)]. The eight isomers of $C_{13}H_9N$ were obtained as follows: acridine, phenanthridine, benzo[*h*]quinoline, and benzo[*f*]quinoline were purchased from Aldrich. Benz[*f*]isoquinoline and benz[*h*]isoquinoline were synthesized via the photochemical cyclization of 3-stilbazole and 4-stilbazole, respectively [C. E. Loader, M. V. Sargent, C. J. Timmons, *Chem. Commun.* **7**, 127 (1965)]. Manuscripts in preparation describe the syntheses of benzo[*g*]quinoline and benz[*g*]-isoquinoline and the embryotoxicity data for all eight isomers.
8. Benzo[*g*]quinoline-5,10-dione was synthesized according to (*4*).
9. The mean weight of the *A. domesticus* egg after water uptake is 606 ± 44 μg. Thus the $LD_{50}$'s of **1** and **2**, expressed as the ratio of chemical weight to egg weight, are 21.7 and 140 mg/kg, respectively.
10. J. S. Edwards and S.-W. Chen, *Wilhelm Roux' Arch. (Dev. Biol.)* **186**, 151 (1979); L. Lauga, *Ann. Sci. Nat. Zool. Biol. Anim.* **11**, 483 (1969); E. Mahr, *Wilhelm Roux' Arch. Entwicklungsmech. Org.* **15**, 662 (1961).
11. B. T. Walton and L. M. Riddiford, unpublished data.
12. B. T. Walton, J. B. Nardi, E. G. O'Neill, unpublished data.
13. We thank A. Bader, Aldrich Chemical Company; G. J. Sloan, E. I. duPont de Nemours and Company; and G. R. Southworth, Oak Ridge National Laboratory, for discussions. Research sponsored by the Office of Health and Environmental Research, U.S. Department of Energy, under contract W-7405-eng-26 with Union Carbide Corporation. This is publication No. 2222, Environmental Sciences Division, Oak Ridge National Laboratory.

1 June 1983; accepted 14 September 1983

## Monoclonal Antibodies in the Lymphatics: Selective Delivery to Lymph Node Metastases of a Solid Tumor

Abstract. *After subcutaneous injection, monoclonal antibodies directed against a tumor can enter local lymphatic vessels, pass to the draining lymph nodes, and bind to metastases there. Lymphatic delivery of antibody to early metastases is more efficient than intravenous administration, and the lymphatic route can be used to image smaller metastatic deposits. Perhaps more important, the lymphatic route minimizes binding of antibodies to circulating tumor antigens and to cross-reactive antigens present on normal tissues. Antibodies inappropriate for intravenous use because of binding to normal tissues may therefore be useful against lymph node metastases when injected subcutaneously or directly into lymphatic vessels.*

Intravenous injection of monoclonal antibodies is being studied in numerous laboratories and hospitals for diagnosis and therapy of cancers (*1*). Antibodies with gamma emitters attached can be used for diagnostic imaging of tumors (*2*). For therapy, antibodies can mark tumor cells for destruction by host defenses (*3*) or carry an attached drug, toxin, radionuclide, or liposome (*4*). We recently reported an alternative to the intravenous route of administration: after subcutaneous injection, monoclonal antibodies enter local lymphatic capillar-

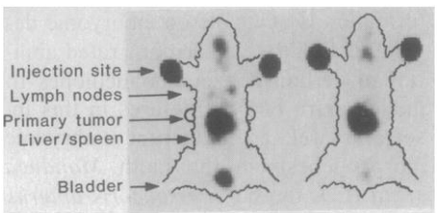


Fig. 1. Gamma camera images of guinea pigs 2½ hours after subcutaneous injection in both front feet with $^{125}$I-labeled D3 antibody. The image on the left is of an animal inoculated bilaterally with $10^6$ L10 tumor cells. At right is a normal animal. Forty thousand counts were recorded with an Anger gamma camera with a low-energy, parallel-hole collimator. Images were smoothed and spontaneous background counts subtracted. Blood pool background was not subtracted. Dose per foot: 3.5 μCi in 200 μl of phosphate-buffered saline with 1 mg of bovine serum albumin per milliliter.

ies, pass to regional lymph nodes, and bind to target cells there (*5*). Antibodies not taken up in the node pass to more distant nodes in the chain and finally enter the systemic circulation, principally through the thoracic duct. In our first study (*5*) the antibodies were directed against *normal* cell types in the node, leaving open the question of whether similar targeting could be achieved with tumors. In this report we describe selective delivery of monoclonal antibodies through the lymphatics to lymph node metastases of a solid tumor. Polyclonal antisera to tumor-associated antigens have previously been localized in the nodes of human patients, but without demonstration of antigenic specificity or proof of localization in the tumor itself (*6*).

For these studies we used guinea pig line 10 (L10) hepatocarcinoma, a chemically induced, transplantable tumor (*7*) that metastasizes to regional lymph nodes and visceral organs. Strain 2 guinea pigs weighing 500 to 600 g were inoculated intradermally in the flank with $10^6$ viable L10 cells. Within 1 week tumor cells metastasized to the ipsilateral superficial distal axillary (SDA) node. We found that antibodies could be delivered by the lymphatic route to that node from the ipsilateral front paw or flank.

The antibody D3 is a murine monoclonal immunoglobulin G1 (IgG1) directed against a dimeric 290,000-dalton antigen on the surface of L10 cells in both primary tumors and metastases (*8*). It does not react with normal tissues of the adult guinea pig, except perhaps smooth muscle (*8*). It accumulates selectively in L10 tumor after intravenous administration (*9*). D3 was purified from ascites by protein A chromatography and labeled with $^{125}$I by the chloramine-T method. It bound to L10 cells in vitro with an affinity of approximately $10^9 M^{-1}$ and a saturation value of approximately $10^6$ IgG molecules per cell.

Figure 1 shows gamma camera images obtained 2½ hours after subcutaneous injection of [$^{125}$I]D3 in the front footpads. SDA nodes were clearly visualized in the guinea pig with tumors but not in the normal animal. Dissection and counting confirmed that the images represented $^{125}$I in the lymph nodes, and, in other experiments, surgical removal of nodes abolished the corresponding images.

The practical limit of sensitivity for the lymphatic approach will depend on such factors as choice of isotope, specific activity, binding parameters of the antibody, and location of the target node with respect to body background. The smallest metastases we imaged were a series of three that constituted 2.3, 4.6, and 5.8 percent of node weight (as estimated by morphometry on paraffin sections cut at three levels in each node). These percentages corresponded to 2.3, 4.0, and 6.7 mg of tumor, respectively. Lymph node tumors must be at least two orders of magnitude larger to be visualized by standard radiographic techniques or computerized tomography (*10*).

The images in Fig. 1 do not prove specificity of binding; nonspecific uptake of antibodies might be greater in hyperplastic nodes draining a tumor or in metastatic deposits than in a normal node. However, we demonstrated specificity by double-labeling with [$^{125}$I]D3 and [$^{131}$I]MOPC 21, the latter being a murine IgG1 with no known binding specificity. Figure 2 shows the radioactivity measured in SDA nodes and in other organs after coinjection of the two antibodies. The ordinate is a dimensionless parameter indicating the tissue concentration of radioactivity, expressed as a fraction of the dose and normalized by the body weight of the animal. This parameter is so defined that all organs would have values of 1.0 if the counts were uniformly distributed throughout the body (without excretion). Nodes ipsilateral to the primary tumor and to the injection showed, on average, a 3.9 to 1 ratio of specific to nonspecific binding. In nodes ipsilateral to the primary tumor but contralateral to the site of injection there were few $^{125}$I counts, in spite of the presence of metastatic tumor in that node. This indicates that delivery to ipsilateral nodes is principally local (through lymphatic drainage, not the bloodstream). "Normal" nodes (contralateral

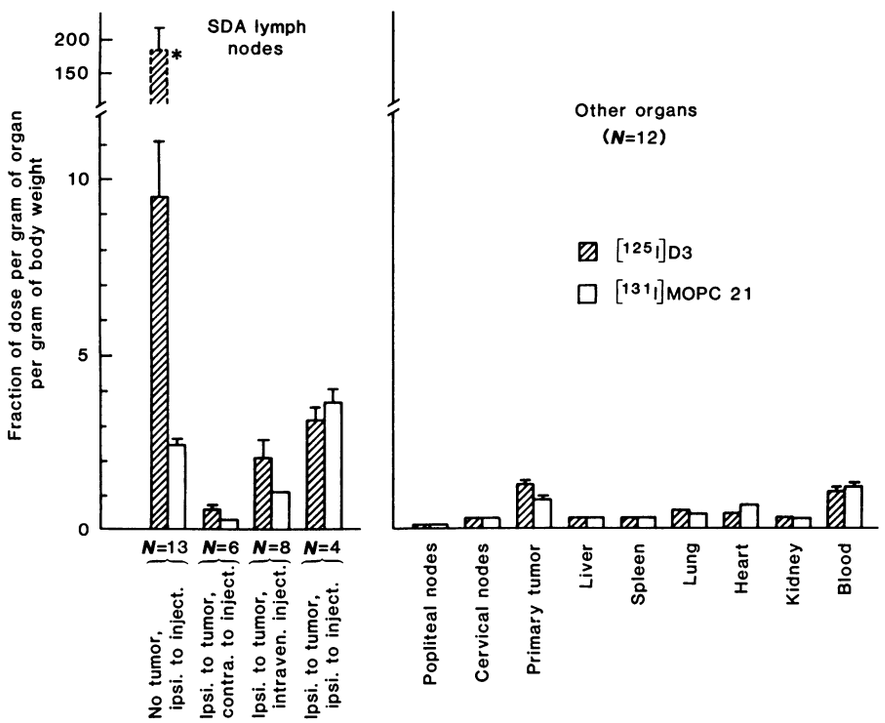


Fig. 2. Distribution of [$^{125}$I]D3 and $^{131}$I-labeled control antibody (MOPC 21) 24 hours after coinjection into guinea pigs with L10 tumors. Injections were subcutaneous in the flank, except where indicated as intravenous. Studies were done 17 to 20 days after implanting $10^6$ L10 tumor cells in the flank. On average, 4 percent of the node weight was tumor. The bar outlined by dashed lines indicates values normalized by tumor weight rather than by node weight (*11*). Injections contained 0.3 μg of [$^{125}$I]D3 (1.9 μCi) and 0.3 μg of [$^{131}$I]MOPC 21 (0.6 μCi) in 200 μl of the medium described in the legend to Fig. 1. The data suggested a proportional error model and hence are expressed as geometric means ± standard errors.

to the primary tumor) on the injection side showed no specific uptake. The popliteal and cervical nodes, which receive antibodies only through the bloodstream, contained few counts and showed no selectivity. There was little or no selectivity in any of the other normal organs. Primary tumors did show a modest selectivity, as expected, but relatively few counts. After intravenous injection, nodes ipsilateral to the tumor contained 4.6 times fewer $^{125}I$ counts than after ipsilateral subcutaneous injection, and the specific to nonspecific ratio was less than 2 to 1.

The specific to nonspecific ratio of 3.9 to 1 quoted for nodes with metastasis and located ipsilateral to the injection is misleadingly low, since at the time of study the metastases were still microscopic. Tumor occupied on average only 4 percent of the node volume, as estimated by morphometry. If the data in Fig. 2 had been normalized by the weight of tumor rather than that of node, the value for D3 in those nodes would have been 180, not 9.5 (*11*). This value is indicated by the dashed bar and asterisk in Fig. 2. The normalized concentration in metastatic tumor was thus approximately 172 times higher than that in blood and 600 times higher than that in liver. Furthermore, the uptake in *normal* nodes ipsilateral to the injection sufficed to account for all of the nonspecific uptake in the cancerous nodes. Hence, the metastases themselves showed a high specific to nonspecific ratio, on the order of 100 to 1.

In the foregoing discussion we tacitly assumed that the specific location of $^{125}I$ in the cancerous node implied binding to tumor. However, antibodies might instead have been binding to antigen shed from the primary tumor and carried down lymphatic vessels to the node. We ruled out that possibility by performing experiments similar to those represented in Fig. 2, but with animals treated as follows: L10 cells were injected bilaterally, but the primary tumor on the left side was excised 9 days after implantation, at which time metastasis had already taken place. Double-label experiments on day 18 then showed equal, selective localization of D3 in the SDA nodes on the two sides.

Localization of D3 in the tumor itself was demonstrated directly by autoradiography. Figure 3, a and c, shows a node with tumor cells along its margin. This pattern reflects a metastatic process in which cells of the primary tumor embolize through lymphatic vessels, enter the subcapsular sinus of the node, lodge in a reticular meshwork there, and grow along the sinus. Only later does tumor infiltrate the parenchyma of the node. As indicated by Fig. 3, b and d, the localization of [$^{125}I$]D3 in the node matched that of tumor cells. Even the small patches of counts along the left-hand margin corresponded to nests of tumor cells visible at higher magnification. There was no tumor elsewhere in the node. The findings were similar for all nodes in the series, whereas cancerous nodes contralateral to the injection showed no such images.

At a later stage of growth (days 24 to 27), the metastases weighed several hundred milligrams and constituted most of the node. Surprisingly, afferent lymphatic vessels had not yet been blocked; antibodies still reached the node and specifically labeled part, though not all, of the tumor there.

Lymphatic delivery has several possible advantages over the intravenous route to the nodes. First, much lower doses may be used for diagnosis or therapy. This may decrease the systemic toxicity of antibodies to which toxins or radionuclides have been conjugated. Second, there is the possibility of imaging smaller masses, with reduced body background. Third, because of the direct entry of antibodies into the lymphatics, node images may appear within minutes after injection (*5*), with no need to await clearance from the bloodstream. Finally, and perhaps most important, compartmental localization will reduce binding of antibodies to antigen shed into the circulation or expressed on normal cells. Our mouse study (*5*) was done with antibodies directed against major histocompatibility antigens expressed on almost all cells in the animal. That system represented the logical extreme of nonspecificity. Nonetheless, images representing less than 1 mg of tissue were obtained. Many monoclonal antibodies derived by immunization against tumor cells have been considered clinically useless because they cross-react with normal tissues. Some antibodies to breast and colon carcinoma, for example, bind to normal epithelia in the breast or gut. Cross-reactive antibodies inappropriate for intravenous use may be effective via the lymphatic route, since they will not encounter competing antigens before reaching the target tumor. If, on the other hand, the antibodies were highly selective and able to circulate for long periods in the bloodstream, multiple passes through blood vessels of the node might make the intravenous route more effective.

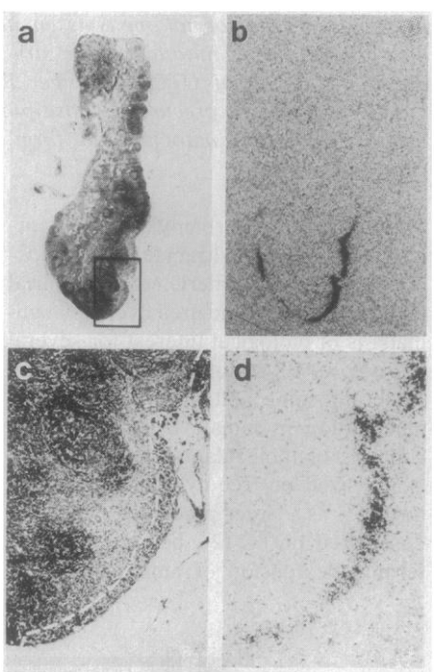


Fig. 3. Autoradiographic study of a cancerous SDA node 24 hours after ipsilateral subcutaneous injection of [$^{125}I$]D3. The guinea pig was injected with 34 μg of D3 (3.4 μCi) 21 days after tumor implantation, in parallel with the experiment represented in Fig. 2. [$^{131}I$]MOPC 21, also injected, was allowed to decay to insignificance before autoradiography. (a) Paraffin-embedded section stained with hematoxylin and eosin. Tumor occupied 2 percent of the node area. (b) Autoradiogram of a 6-μm section cut adjacent to the section shown in (a). Grains representing [$^{125}I$]D3 are seen along the rim of the node at one end. (c) Higher magnification view corresponding to the inset in (a). Large, pleomorphic tumor cells occupy the area demarcated by white dashed line. (d) Autoradiogram of a section cut adjacent to that shown in (c). Magnifications: ×14 (a and b) and ×57 (c and d).

The most serious limitation of lymphatic delivery is its restriction to lymph nodes that drain the site of injection. One can, however, identify several clinical settings in which the approach may prove useful. Assessment of lymph node status is important in determining the stage of numerous malignancies, among them Hodgkin's disease, malignant melanoma, and the carcinomas of breast, testis, lung, colon, cervix, and prostate (*12*). Information on the nodes can be used in selecting patients for adjuvant therapy (as with breast cancer) or in determining the fields to be irradiated (as with testicular and cervical carcinomas). Standard lymphangiographic studies with radiopaque emulsions require cannulation of the lymphatic vessels; monoclonal antibodies could be administered in the same way, but the present study suggests that they are sufficiently well mobilized after simple subcutaneous injection. If so, the technique may reach node groups not opacified by standard lymphangiography.

Therapeutic use of monoclonal anti-

bodies by the lymphatic route is more speculative, but conventional therapy suggests several possibilities. Irradiation of regional nodes may improve the prognosis for patients with tumors spread predominantly through the lymphatics, for example in selected cases of Hodgkin's disease, non-Hodgkin's lymphoma, and seminomatous testicular carcinoma (*12*). Lymphatic flow might be distorted or blocked by large lymph node masses, but for occult metastases of such tumors, adjuvant therapy with antibodies delivered through the lymphatics could prove effective.

JOHN N. WEINSTEIN
MICHAEL A. STELLER
*Laboratory of Theoretical Biology, National Cancer Institute, National Institutes of Health, Bethesda, Maryland 20205*
ANDREW M. KEENAN
*Department of Nuclear Medicine, Clinical Center, National Institutes of Health*
DAVID G. COVELL
*Laboratory of Theoretical Biology, National Cancer Institute*
MARC E. KEY*
*Cancer Metastasis and Treatment Laboratory, NCI–Frederick Cancer Research Facility, Frederick, Maryland 21701*
SUSAN M. SIEBER
*Office of the Director, Division of Cancer Cause and Prevention, National Cancer Institute*
ROBERT K. OLDHAM
KOU M. HWANG
*Biological Response Modifiers Program, NCI–Frederick Cancer Research Facility*
ROBERT J. PARKER
*Office of the Director, Division of Cancer Cause and Prevention, National Cancer Institute*

### References and Notes

1. L. L. Houston, R. C. Nowinski, I. D. Bernstein, *J. Immunol.* **125**, 837 (1980); M. R. Tam, I. D. Bernstein, R. C. Nowinski, *Transplantation* **33**, 269 (1982); G. N. Sfakianakis and F. H. DeLand, *J. Nucl. Med.* **23**, 840 (1982).
2. G. Levine *et al.*, *J. Nucl. Med.* **21**, 570 (1980); D. A. Scheinberg, M. Strand, O. A. Gansow, *Science* **215**, 1511 (1982); D. M. Goldenberg and F. H. DeLand, *J. Biol. Response Modif.* **1**, 121 (1982).
3. R. A. Miller, D. G. Maloney, R. Warnke, R. Levy, *N. Engl. J. Med.* **306**, 517 (1982).
4. K. A. Foon, M. I. Bernhard, R. K. Oldham, *J. Biol. Response Modif.* **1**, 277 (1982); J. N. Weinstein, in *Rational Basis for Chemotherapy*, B. A. Chabner, Ed. (Liss, New York, 1982), p. 441.
5. J. N. Weinstein *et al.*, *Science* **218**, 1334 (1982).
6. S. E. Order *et al.*, *Cancer (Philadelphia)* **35**, 1487 (1975); F. H. DeLand *et al.*, *J. Nucl. Med.* **20**, 1243 (1979). For critique and reply, see G. N. Ege and M. J. Bronskill [*ibid.* **21**, 804 (1980)] and F. H. DeLand, E. E. Kim, and D. M. Goldenberg [*ibid.*, p. 805].
7. H. J. Rapp *et al.*, *J. Natl. Cancer Inst.* **41**, 1 (1968).
8. M. I. Bernhard *et al.*, *Cancer Res.* **43**, 4420 (1983).
9. M. E. Key *et al.*, *J. Immunol.* **130**, 1451 (1983); M. I. Bernhard *et al.*, *Cancer Res.* **43**, 4429 (1983).
10. G. D. Moak, E. M. Cockerill, M. O. Farber, P. B. Yaw, F. Manfredi, *Chest* **82**, 69 (1982).
11. The dimensionless concentration of D3 defined per unit volume of metastatic tumor ($C^{D3}_t$) and that defined per unit volume of node including tumor ($C^{D3}_n$) are related approximately by the expression $C^{D3}_t = (C^{D3}_n)/\beta$, where $\beta$ is the volume fraction occupied by tumor. A correction can be made for D3 in nontumor areas of the node by assuming (i) that D3 and MOPC 21 are distributed equally in nontumor areas of cancerous nodes, as they are in normal nodes (Fig. 2), (ii) that MOPC 21 is distributed equally between tumor and nontumor areas, and (iii) that MOPC 21 accurately reflects the nonspecific accumulation of D3. Then, $C^{D3}_t = [C^{D3}_n - C^{MOPC}_n(1 - \beta)]/\beta$. For the mean values from Fig. 2, with the geometric mean of $\beta$ equal to 0.04, we have $C^{D3}_t = (9.5 - 2.4 \times 0.96)/0.04 = 180$.
12. See, for example, V. T. De Vita, Jr., S. Hellman, S. A. Rosenberg, *Cancer: Principles and Practice of Oncology* (Lippincott, Philadelphia, 1982).
13. We thank M. J. Talley and C. Botkin for valuable technical assistance; R. Blasberg, E. Owens, and M. Juhler for help with the autoradiography; K. A. Foon and M. I. Bernhard for advice and assistance with the L10 tumor and D3 antibodies; and G. Morstyn and E. Glatstein for critical reading of the manuscript.
* Present address: Center for Biochemical and Biophysical Sciences in Medicine, Harvard Medical School, Boston, Mass. 02115.

11 July 1983

## Biogenesis of Ornithine Transcarbamylase in *spf*$^{ash}$ Mutant Mice: Two Cytoplasmic Precursors, One Mitochondrial Enzyme

Abstract. *Extracts of liver from hemizygous affected mice with the X-linked* spf$^{ash}$ *mutation have 5 to 10 percent of normal ornithine transcarbamylase (OTC) activity, yet the homogeneous enzyme isolated from these extracts is identical to that in controls. The OTC messenger RNA from mutant livers programs the synthesis of two distinct OTC precursor polypeptides—one normal in size, the other distinctly elongated. Both precursors are imported and proteolytically processed by mitochondria, but only the normal one is assembled into active trimer. This novel phenotype may result from a mutation in the structural gene for OTC leading, primarily, to aberrant splicing of OTC messenger RNA and, secondarily, to formation of a structurally altered precursor whose posttranslational pathway is ultimately futile because its mature mitochondrial form is not capable of assembly and functional expression.*

Ornithine transcarbamylase (OTC; ornithine carbamoyltransferase; E.C. 2.1.3.3), a homotrimeric, mitochondrial matrix enzyme of the urea cycle in mammals, is of biological interest for several reasons. (i) Its structural locus is on the X chromosome and undergoes random inactivation in female cells (*1*); (ii) its subunit, of molecular size ~36 kD, is synthesized on free cytoplasmic polyribosomes as a larger precursor (~40 kD), designated pOTC (*2*), bearing an $NH_2$-terminal extension of amino acid residues (*3*), which is cleaved proteolytically concomitant with its posttranslational energy-dependent import by mitochondria (*4–6*); (iii) it is expressed almost exclusively in hepatocytes (*1*); and (iv) its inherited deficiency in man often produces lethal ammonia intoxication in affected males (*1*).

Our understanding of the nature and significance of mutations at the human OTC locus has been enhanced by the recent description of two X-linked, allelic OTC mutants in mice (*7*, *8*). One, designated *spf* (sparse fur) is almost certainly a point mutation, which affects the active site of OTC. When assayed in vitro, hepatic OTC activity in *spf* mice is reduced to ~20 percent of control at physiologic *p*H (*7*, *9*, *10*), affinity for

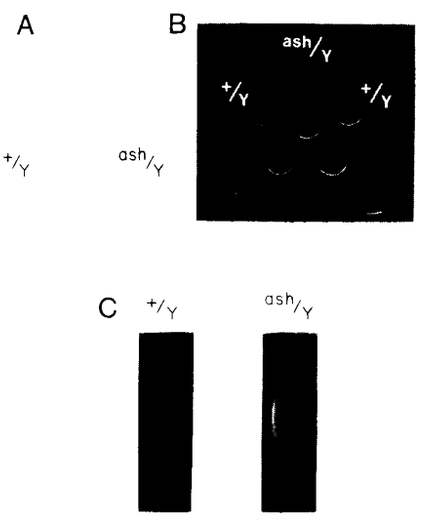


Fig. 1. Characteristics of homogeneous OTC from livers of +/Y and *spf*$^{ash}$/Y mice. (A) SDS-PAGE; enzymes (6 μg) were applied to SDS-polyacrylamide (10 percent) gel slabs after denaturation with 2-mercaptoethanol and SDS; the gel was stained with Coomassie blue. (B) Ouchterlony double diffusion in agar; 6 μl of rabbit antiserum to rat OTC was placed in the center well, and 1- to 2-μg of respective OTC's was added to the outer wells. (C) Immunoelectrophoresis; 4 μg of enzyme from +/Y or *spf*$^{ash}$/Y liver was placed in the wells; after electrophoresis, 200 μl of rabbit antiserum to rat OTC was placed in the channels and developed overnight.